

# Spin Order by Frustration in Triangular Lattice Mott Insulator $\text{NaCrO}_2$ : A Neutron Scattering Study

D. Hsieh,<sup>1,2</sup> D. Qian,<sup>1,3</sup> R. F. Berger,<sup>4</sup> Chang Liu,<sup>1</sup> B. Ueland,<sup>5</sup>  
P. Schiffer,<sup>5</sup> Q. Huang,<sup>6</sup> R. J. Cava,<sup>4</sup> J. W. Lynn,<sup>6</sup> and M. Z. Hasan<sup>1</sup>

<sup>1</sup>*Joseph Henry Laboratories of Physics, Princeton University, Princeton, New Jersey 08544, USA*

<sup>2</sup>*(Present Address)Institute for Quantum Information and Matter,  
California Institute of Technology, Pasadena, California 91125, USA*

<sup>3</sup>*(Present Address)Department of Physics and Astronomy,  
Shanghai Jiao Tong University, Shanghai 200240, China*

<sup>4</sup>*Department of Chemistry, Princeton University, Princeton, New Jersey 08544, USA*

<sup>5</sup>*Department of Physics, Pennsylvania State University, University Park, Pennsylvania 16802, USA*

<sup>6</sup>*NIST Center for Neutron Research, Gaithersburg, Maryland 20899, USA*

(Dated: October 13, 2018)

We report high resolution neutron scattering measurements on the triangular lattice Mott insulator  $\text{Na}_x\text{CrO}_2$  ( $x=1$ ) which has recently been shown to exhibit an unusually broad fluctuating crossover regime extending far below the onset of spin freezing ( $T_c \sim 41\text{K}$ ). Our results show that below some crossover temperature ( $T \sim 0.75T_c$ ) a small incommensuration develops which helps resolve the spin frustration and drives three-dimensional magnetic order supporting coherent spin wave modes. This incommensuration assisted dimensional crossover suggests that inter-layer frustration is responsible for stabilizing the rare 2D correlated phase above  $0.75T_c$ . In contrast to the host compound of 2D cobaltate superconductor such as  $\text{Na}_x\text{CoO}_2$  ( $\xi_c > 50\text{\AA}$ ), no magnetic long-range order is observed down to  $1.5\text{K}$  ( $\xi_c < 16\text{\AA}$ ).

Two dimensional (2D) systems such as rare-gas atoms adsorbed on graphite [1], quantum wells [2] or graphite intercalation compounds [3] are routinely engineered in the laboratory to search for spontaneously emerging 2D correlated phases. However spontaneous emergence of a 2D correlated phase in a bulk 3D system is rare and can arise because of geometrical frustration. Specific examples are the square lattice antiferromagnets (AFM) belonging to the rare-earth copper-oxides [4], and the spin dimer system  $\text{BaCuSi}_2\text{O}_6$  [5]. Recent discoveries of possible low temperature spin liquid phases in  $\text{Cs}_2\text{CuCl}_4$  [6] and  $\text{NiGa}_2\text{S}_4$  [7], a rich phase diagram for  $\text{Na}_x\text{CoO}_2$  [8], and exotic multiferroic behavior in  $\text{ACrO}_2$  systems [9, 10] have generated interest in whether geometrical frustration might stabilize novel 2D phases on stacked triangular lattices (TL). Such a state has been theoretically proposed to realize the long sought  $Z_2$  topological vortex phase [11].

Early neutron diffraction work on the TL Mott insulator  $\text{NaCrO}_2$  demonstrated highly anisotropic magnetic correlations developing near  $T \sim 45\text{K}$  which persist down to  $2\text{K}$  [12]. Recent  $\mu\text{SR}$  and NMR measurements [13] reveal an onset of gradual spin freezing at  $T_c \sim 41\text{K}$ , followed by an unusually broad fluctuation regime that reaches a maximal spin relaxation rate at  $0.75T_c$ . Although strong fluctuations are a hallmark of highly frustrated systems, the relationship between frustration and the 2D static behavior is unknown because detailed knowledge of the magnetic structure is lacking. Here we study the temperature evolution of both the static and dynamic spin correlations with high resolution neutron scattering measurements, and find that inter-layer frustration is essential for stabilizing the rare 2D antiferromagnetically correlated phase in  $\text{NaCrO}_2$ .

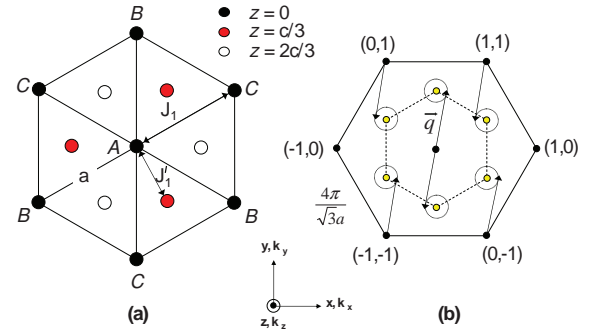


FIG. 1: Crystal structure of  $\text{NaCrO}_2$ . The  $R\bar{3}m$  crystal symmetry of  $\text{NaCrO}_2$  was verified at both  $300\text{K}$  and  $4\text{K}$  by Rietveld refinement of high resolution neutron powder diffraction data. Lattice constants at  $4\text{K}$  are  $a = 2.968\text{\AA}$  and  $c = 15.944\text{\AA}$ . (a)  $[001]$  view of Cr sublattice. The in-plane  $J_1$  and inter-plane  $J_1'$  exchange paths are marked, as well as the three-sublattice ( $ABC$ ) structure corresponding to  $\vec{q} = (0, 4\pi/3a, 0)$ . (b) Reciprocal lattice of hexagonal crystal structure (black dots) and three-sublattice magnetic structure (yellow dots). Measured low temperature  $\vec{q}$  (arrows) deviates slightly from  $(0, 4\pi/3a, 0)$ .

The classical ground state of the nearest neighbor TLAFM is the  $120^\circ$  spin structure. If such layers are rhombohedrally stacked [fig. 1(a)], there is a cancellation of inter-layer Weiss fields which leads to a classical decoupling of spin layers. The  $\text{ACrO}_2$  ( $A=\text{Li, Na, K}$ ) partially-filled band Mott insulators, in which  $\text{Cr}^{3+}$  ( $S = \frac{3}{2}$ ) ions form a rhombohedrally stacked TL [fig. 1(a)], are good candidates for the physical realization of such a system.

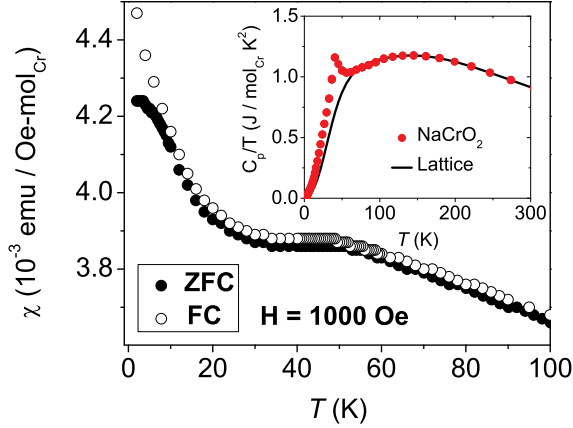


FIG. 2: Susceptibility and specific heat. Field cooled (FC) and zero-field cooled (ZFC) susceptibility  $\chi$  measured at 1000 Oe with a SQUID magnetometer (Q.D. MPMS). Inset: Specific heat divided by temperature  $C_p/T$  of NaCrO<sub>2</sub> measured in a commercial apparatus (Q.D. PPMS) in zero magnetic field. The magnetic contribution is obtained by subtracting out the estimated lattice contribution (solid line) based on non-magnetic NaScO<sub>2</sub>. 1 emu/(mol Oe) =  $4\pi \cdot 10^{-6}$  m<sup>3</sup>/mol.

The CrO<sub>2</sub> layers are isostructural with the CoO<sub>2</sub> layers in superconducting Na<sub>x</sub>CoO<sub>2</sub>·yH<sub>2</sub>O [14], and adjacent layers are well separated by intervening A ions, suggesting predominant 2D behavior in the *ab* plane. Detailed neutron scattering studies have only been made on LiCrO<sub>2</sub>, which orders 3D at low temperature [15].

A 15g powder sample of NaCrO<sub>2</sub> was prepared using the method described in [13]. The d.c. susceptibility  $\chi$  of NaCrO<sub>2</sub> measured up to 350K (fig. 2) is consistent with earlier work up to 800K [16]. The Curie-Weiss temperature  $\Theta_{CW} \sim -280$ K obtained from the latter study yields an estimate of  $J_1 + J'_1 = [3k_B\Theta_{CW}/zS(S+1)] \sim -3$  meV, where  $z = 6$  is both the in-plane and inter-plane coordination number. The effective magnetic moment is close to the spin-only value of  $3.87\mu_B$  for spin- $\frac{3}{2}$  Cr<sup>3+</sup>. The maximum in  $\chi$  around 48 K is broad and weakly temperature dependent, and is similarly seen in theoretical simulations of model 2D TLA FM's [17]. We were able to rule out a spin-glass transition at this temperature based on the absence of splitting between the field cooled (FC) and zero-field cooled (ZFC) curves. Moreover, a.c. susceptibility measurements showed no frequency depen-

dence of this maximum, implying a single relaxation time scale. The low temperature upturn and splitting in  $\chi$  is likely due to freezing of vacancy or grain boundary spins.

The magnetic specific heat,  $C_M(T)$ , (inset fig. 2) shows a broad maximum at 40 K, slightly below the maximum in  $\chi(T)$ . The positions of these two features are much reduced from  $\Theta_{CW}(\sim -280$ K), which reflects a geometrical frustration ( $f \sim 7$ ) induced spectral weight downshift. Unlike the specific heat of directly stacked quasi-2D TLA FM's of type VX<sub>2</sub> ( $X = \text{Cl, Br}$ ) [18], which show a sharp lambda-type anomaly coincident with 3D magnetic ordering, the specific heat maximum of NaCrO<sub>2</sub> is very broad [19].

Magnetic neutron scattering was performed at the NIST Center for Neutron Research. This probes the spherically averaged scattering function  $S^{\alpha\beta}(\vec{Q}, \omega)$  [20]

$$I(Q, \omega) = r_0^2 \frac{g}{2} |F(Q)|^2 \int \frac{d\Omega_{\hat{Q}}}{4\pi} \sum_{\alpha\beta} (\delta_{\alpha\beta} - \hat{Q}_\alpha \hat{Q}_\beta) S^{\alpha\beta}(\vec{Q}, \omega) \quad (1)$$

where  $r_0 = 5.38$  fm,  $F(Q)$  is the magnetic form factor for Cr<sup>3+</sup> and  $g$  is the Landé  $g$ -factor. Diffraction scans were measured on the BT2 triple-axis spectrometer with a fixed incident and final energy of 14.7 meV. We used PG (002) reflections for both the monochromator and the analyzer, and horizontal beam collimations of 60'-40'-40'-open. The magnetic contribution,  $I(Q)$ , was obtained by subtracting the 100 K data, and was normalized to the nuclear peaks (fig. 3). All magnetic peaks were resolution limited in energy ( $\delta E = 0.07$  meV), which implies that spin correlations persist on a time scale that exceeds 0.4 ns.

The data were fit to a convolution of a Gaussian instrumental resolution ( $\delta Q = 0.03 \text{ \AA}^{-1}$ ) with the spherical average of magnetic scattering from a quasi-2D magnet. This is described by a Warren function with an additional phase factor [4] (see eq. 2), where  $C$  is an instrumental constant,  $\vec{q}_{\parallel}$  and  $\vec{q}_{\perp}$  are the components of the ordering wave vector parallel and perpendicular to the triangular planes respectively, and the sum is over 2D reciprocal lattice vectors  $\vec{\tau}$  [fig. 1(b)]. The ordered moment on a site  $\vec{r}$  is given by  $\vec{m}_{\vec{q}} e^{i\vec{q}\cdot\vec{r}} + \vec{m}_{\vec{q}}^* e^{-i\vec{q}\cdot\vec{r}}$  where  $\vec{m}_{\vec{q}} = (im_{qx}, m_{qy}, m_{qz})$ . The number of correlated layers  $N$  was restricted to integer values, with  $\vec{d} = (a/(2\sqrt{3}), a/2, c/3)$  being a vector connecting adjacent layers.

$$I(Q) = C \frac{|F(Q)|^2}{Q} \sum_{\vec{\tau}} \int_{-\frac{\pi}{2}}^{\frac{\pi}{2}} (|\vec{m}_{\vec{q}}|^2 - |\hat{Q} \cdot \vec{m}_{\vec{q}}|^2) \times e^{-\frac{\xi_{ab}^2}{4\pi} (Q \cos \phi - |\vec{\tau} \pm \vec{q}_{\parallel}|)^2} \left| \sum_{n=0}^{N-1} e^{in[\vec{\tau} \cdot \vec{d}_{\parallel} + (Q \sin \phi + q_{\perp}) d_{\perp}]} \right|^2 d\phi \quad (2)$$

Before discussing the fit results, it is worth pointing

out some differences between the powder lineshapes of

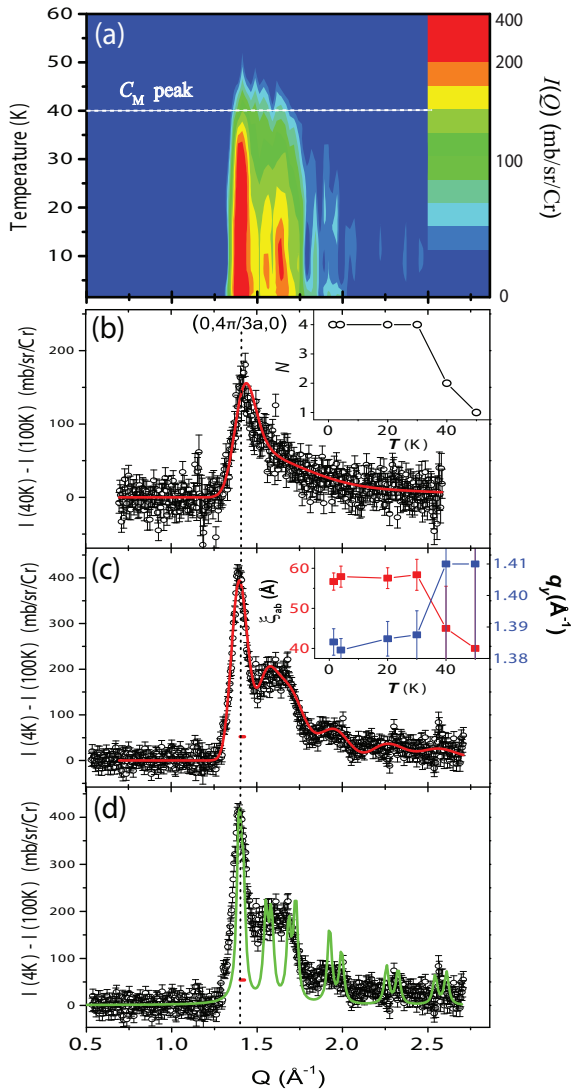


FIG. 3: Quasi-static spin correlations. (a) Neutron thermodiffractogram measured using a disk-chopper spectrometer. Intensity is displayed on a log scale to enhance the high  $Q$  features. Dashed line indicates peak position of magnetic specific heat  $C_M$ . (b) 40 K and (c) 4 K magnetic diffraction measured in triple-axis mode using 100 K background. Red curves are fits using methods described in the text, and the red bar indicates the FWHM resolution width. Inset (b): Value of  $N$  that minimized  $\chi^2$  at each temperature. Inset (c): Temperature dependence of  $\xi_{ab}$  and  $q_y$ . The green curve in (d) is a calculated resolution limited lineshape assuming spins are 3D long-range ordered with the fitted  $\vec{q}$ . Uncertainties are statistical in origin and represent one standard deviation.

directly stacked and rhombohedrally stacked quasi-2D TLA FM's. Coherent scattering from a single layer of  $120^\circ$  correlated spins comes from the intersection of a spherical shell of radius  $Q$  in reciprocal space with Bragg rods centered at  $\vec{\tau} \pm \vec{q}$ , where  $\vec{q} = (0, 4\pi/3a, 0)$  (fig. 1). For  $N=1$  the intensity along each rod is uniform, which pro-

duces the well known saw-tooth lineshape. For  $N > 1$ , an additional phase factor in eq. 2 generates an oscillatory intensity with period  $2\pi/d_\perp = 6\pi/c$  along the rods. Since  $\vec{d}_\parallel = 0$  for direct stacking, the phase factor is independent of  $\vec{\tau}$  and modulations of the saw-tooth pattern are visible as soon as  $N > 1$  (see, e.g.,  $\text{NiGa}_2\text{S}_4$  [7]). For rhombohedral stacking on the other hand, each rod acquires an additional offset  $(\vec{\tau} \cdot \vec{d}_\parallel)/d_\perp = 0, 2\pi/c$  or  $4\pi/c$  depending on the rod position [fig. 1(b)]. If intensity modulations along an individual rod are sufficiently broad, they will be washed out when averaged over different rods. Therefore the scattering profile can still have a pure saw-tooth shape even for  $N > 1$ .

Least  $\chi^2$  fit results are shown in fig. 3(b) and (c). For  $T > 40\text{K}$  spin correlations are purely 2D ( $N=1$ ). Weak inter-plane correlations develop at 40K ( $N=2$ ) and  $N$  saturates to 4 from 30K down to 1.5K. A comparison of the 1.5K data to the expected lineshape in the limit  $N \rightarrow \infty$  [fig. 3(d)] shows that  $\xi_c$  is indeed short-range. Moreover, all  $(00l)$  nuclear peaks were resolution limited, which suggests that this effect is not due to structural disorder. The in-plane correlation length  $\xi_{ab}$  also increases abruptly between 50K and 30K, corresponding to 13 and 20 triangular lattice spacings respectively, and remains constant upon further cooling. The data at all temperatures show spins confined to the  $xz$ -plane (i.e.  $m_{qy} \ll m_{qx}, m_{qz}$ ), which is consistent with electron paramagnetic resonance (EPR) results supporting a small easy-axis anisotropy [21]. The average ordered moment at 1.5K is estimated to be  $\langle S^2 \rangle \approx (3/2) \int_{1\text{\AA}^{-1}}^{2.5\text{\AA}^{-1}} [I(Q)/(r_0^2 |F(Q)|^2)] Q^2 dQ / \int_{1\text{\AA}^{-1}}^{2.5\text{\AA}^{-1}} Q^2 dQ = 0.55(2)/\text{Cr}$  or  $\sqrt{\langle S^2 \rangle} = 0.74(1)$  which is substantially reduced from  $S=1.5$ .

The development of weak  $c$ -axis correlations between 40K and 30K is accompanied by a change in  $\vec{q}$  [inset fig. 3(c)] from  $(0.0(0), 1.41(5), 0.0(0)) \approx (0, 1.411, 0) = (0, 4\pi/3a, 0)$  to  $(0.03(1), 1.38(1), 0.15(2))$  respectively, and remains fairly constant down to 1.5K [inset fig. 3(c)]. The ordering wave vector at 40K points to a  $120^\circ$  arrangement, and is consistent with the purely 2D nature of spin correlations and the absence of a difference signal in the  $Q \rightarrow 0$  limit at this temperature. The slight incommensuration at 30K represents a departure from  $120^\circ$  order which resolves the inter-layer frustration to some extent, and naturally explains the onset of inter-layer correlations. This supports recent  $\mu\text{SR}$  and NMR data [13] which reveal the start of an extended crossover regime at 41K and a maximal spin relaxation rate near 30K.

The classical ground state  $\vec{q}$  of a rhombohedrally stacked TLA FM including only  $J_1$  and  $J'_1 < 3J_1$  was shown by Rastelli *et al* [22] to be infinitely degenerate along helices given by  $((-2j'/\sqrt{3}a) \sin(cq_z/3), 4\pi/3a + (2j'/\sqrt{3}a) \cos(cq_z/3), q_z)$ , where  $j' \equiv J'_1/J_1$ . Quantum fluctuations select the discrete set  $q_z = 2n\pi/c$  ( $(2n+1)\pi/c$ ) for  $j'$  positive (negative), where  $n$  is an integer. The  $\vec{q}$  extracted

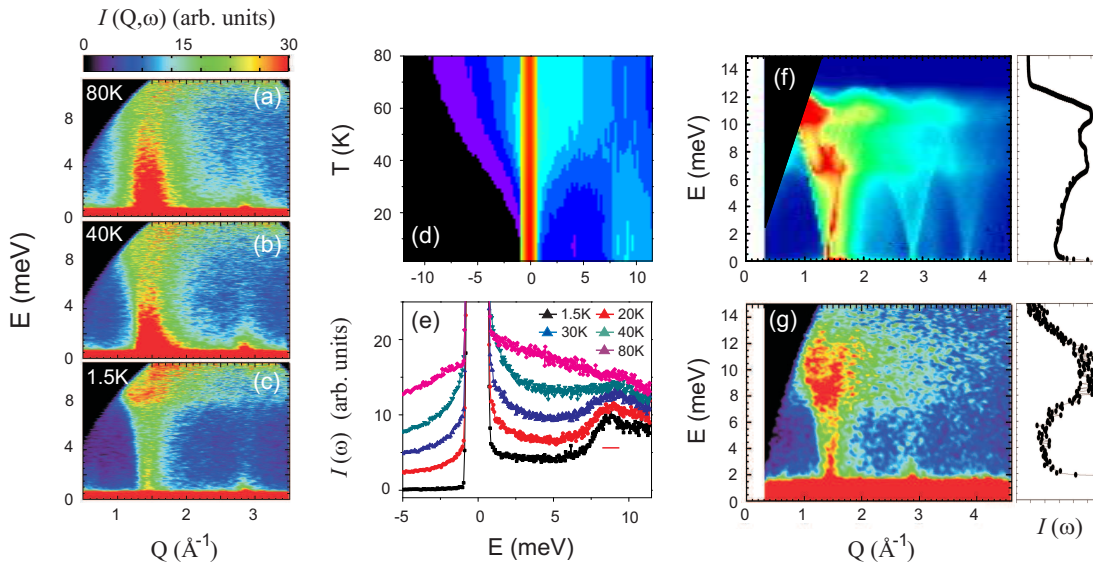


FIG. 4: Dynamic spin correlations. (a)-(c) Neutron scattering data  $I(Q, \omega)$  using 2.5 Å incident neutrons. Panels (d) and (e) show the temperature dependence of the magnetic density of states  $I(\omega) = \int_{-1A}^{2A} I(Q, \omega) dQ$ . Horizontal bar shows instrument energy resolution. Panel (g) shows neutron scattering data taken at 1.5 K measured using 1.8 Å incident neutrons, and panel (f) shows the corresponding linear spin wave calculation.

from data below 30K lies on the degenerate helix if one takes  $j' \sim -0.1$ . Contrary to [13], this result suggests that inter-layer coupling is driven by exchange ( $J'_1 \sim 0.3$  meV) as opposed to  $\text{Cr}^{3+}$  dipolar energies  $(3.8\mu_B)^2/d^3 \sim 0.06$  meV. The fitted  $q_z$  value 0.15(2) is close to  $\pi/c = 0.197$  which is consistent with  $j' < 0$ . Therefore quantum order-by-disorder may be responsible for the single- $\vec{q}$  low temperature magnetic structure.

Magnetic neutron inelastic scattering experiments were performed on the Disk Chopper Spectrometer (DCS) using 1.8 Å and 2.5 Å incident neutrons. Typical data sets are shown in fig. 4(a)-(c). For  $T > 40\text{K}$ , there is a cooperative paramagnetic continuum centered at  $Q=1.4 \text{ \AA}^{-1}$  due to fluctuations of small  $120^\circ$ -type clusters, which is a prominent feature of triangular frustrated magnets [23]. At 40K, there is an upward shift in the magnetic density of states [fig. 4(e)], obtained by integrating  $I(Q, \omega)$  over a  $1 \text{ \AA}^{-1}$  window about  $Q=1.4 \text{ \AA}^{-1}$ . Surprisingly, despite a large  $\xi_{ab}$  of 45 Å, most of the inelastic scattering weight remains in the incoherent channel suggesting heavily damped spin wave modes. Only below 30K, where short-range  $c$ -axis correlations have been established, do dispersive excitations appear.

In order to make contact with diffraction results, we carried out a linear spin wave calculation of  $I(Q, \omega)$  [6] for a system following the Hamiltonian:

$$H = -J_1 \sum_{ab_{nn}} \vec{S}_i \cdot \vec{S}_j - J'_1 \sum_{c_{nn}} \vec{S}_i \cdot \vec{S}_j \quad (3)$$

where  $ab_{nn}$  and  $c_{nn}$  denote nearest in-plane and inter-

plane neighbors respectively,  $J_1 = -2.4$  meV (AFM),  $J'_1 = 0.24$  meV (FM),  $\vec{q} = (0.03, 1.39, 0.15)$ ,  $S = \frac{3}{2}$  and spins were confined to the  $xz$ -plane. The result shown in fig. 4(f) reproduces the main features of the low temperature spectrum, as well as the two maxima in the density of states. However, while there is agreement in the position of the high energy maximum around 11 meV, the calculated position of the low energy maximum falls short of the data by about 2 meV. This deficit can be accounted for by including an easy-axis anisotropy term  $D$ , as shown by previous numerical studies [24], albeit with a  $D$  value significantly larger than that deduced from EPR measurements at 300K. One possible reason for this discrepancy is that the single-ion  $D$  increases significantly upon cooling, which can also explain the dynamical crossover behavior at 40K [13]. Alternatively, more exotic mechanisms such as a fluctuation induced spin wave gap can be at play (see, e.g.,  $\text{Sr}_2\text{Cu}_3\text{O}_4\text{Cl}_2$  [25]). The *effective* exchange energy  $J_1 + J'_1$  obtained from spin wave analysis is reduced by approximately 25% compared to its *bare* value obtained from  $\chi$ . This large downward renormalization is consistent with theoretical results for the  $S=1/2$  2D TLA FM [26].

To conclude, our neutron scattering measurements clearly reveal a rare 2D antiferromagnetic phase in  $\text{NaCrO}_2$  with strong spin fluctuations over an extended temperature range. The development of  $c$ -axis correlations at low temperature together with a weak incommensurate modulation strongly suggest inter-layer frustration as the mechanism for the stability of this unusual 2D phase. Such a 2D magnetic phase of Mott insulators

can be a host for exotic superconductors where pairing could be mediated by the naturally available spin fluctuations or the lifted zero-modes unique to frustrated systems and would make an interesting variant of the recently discovered cobaltate superconductor hydrated  $\text{Na}_x\text{CoO}_2$ .  $\text{NaCrO}_2$  has also been recently shown to be a

host for an unusual spin-driven antiferroelectric phase [9], which will provide important insight into how magnetic frustration can give rise to strong coupling multiferroic behavior [10]. Quite generally, our results demonstrate that geometrical frustration provides a new avenue to stabilize 2D bulk phases of matter.

- 
- [1] R.J. Birgeneau and P.M. Horn, *Science* **232**, 329 (1986).  
 [2] H. Manoharan *et al.*, *Phys. Rev. Lett.* **77**, 1813 (1996); K. von Klitzing, *Rev. Mod. Phys.* **58**, 519 (1986).  
 [3] D.G. Wiesler *et al.*, *Phys. Rev.* **B36**, 7051 (1987).  
 [4] H. Zhang *et al.*, *Phys. Rev.* **B41**, 11229 (1990); S.Y. Wu *et al.*, *Phys. Rev.* **B54**, 10019 (1996).  
 [5] S.E. Sebastian *et al.*, *Nature* **441**, 617 (2006).  
 [6] R. Coldea *et al.*, *Phys. Rev.* **B68**, 134424 (2003).  
 [7] S. Nakatsuji *et al.*, *Science*. **309**, 1697 (2005).  
 [8] M.L. Foo *et al.*, *Phys. Rev. Lett.* **92**, 247001 (2004); G. Gasparovic *et al.*, *Phys. Rev. Lett.* **96**, 046403 (2006).  
 [9] S. Seki *et al.*, cond-mat/0801.3757 preprint, (2008).  
 [10] S.-W. Cheong and M. Mostovoy, *Nature Mat.* **6**, 13 (2007).  
 [11] H. Kawamura and A. Yamamoto, *J. Phys. Soc. Jpn.* **76**, 073704 (2007).  
 [12] J.L. Soubeyroux *et al.*, *J. Magn. Magn. Mater.* **14**, 159 (1979).  
 [13] A. Olariu *et al.*, *Phys. Rev. Lett.* **97**, 167203 (2006).  
 [14] K. Takada *et al.*, *Nature* **422**, 53 (2003); R.E. Schaak *et al.*, *Nature (London)* **424**, 527 (2003).  
 [15] H. Kadowaki *et al.*, *J. Phys.: Condens. Matter* **7**, 6869 (1995).  
 [16] C. Delmas *et al.*, *J. Phys. Chem. Solids* **39**, 55 (1978).  
 [17] Y. Oohara *et al.*, *J. Phys. Soc. Jpn.* **53**, 4138 (1984).  
 [18] J. Wosnitza *et al.*, *J. Phys.: Condens. Matter* **6**, 8045 (1994).  
 [19] There is no violation of the Mermin-Wagner theorem since there is no sign of a phase transition in  $C_p(T)$ .  
 [20] S.W. Lovesey, *Theory of Neutron Scattering from Condensed Matter*, vol. 2 (Clarendon Press, Oxford, 1984).  
 [21] P.R. Elliston *et al.*, *J. Phys. Chem. Solids* **36**, 877 (1975).  
 [22] E. Rastelli *et al.*, *J. Phys. C: Solid State Phys.* **20**, L303 (1987).  
 [23] T.J. Sato *et al.*, *Phys. Rev.* **B68**, 104432 (2003).  
 [24] Y. Watabe *et al.*, *Phys. Rev.* **B52**, 3400 (1995). We were unable to calculate  $S^{\alpha\beta}(\vec{Q}, \omega)$  including a  $D$  term because the spin wave dispersion becomes non-analytic.  
 [25] Y.J. Kim *et al.*, *Phys. Rev. Lett.* **83**, 852 (1999).  
 [26] O.A. Starykh *et al.*, *Phys. Rev.* **B74**, 180403(R) (2006).